Journal of Mechanical Engineering and Automation 2016, 6(3): 65-70
DOI: 10.5923/j.jmea.20160603.04

Natural Convection in Inclined Wavy-Wall Cavity Filled with Al_2O_3-water Nanofluid using Heatline Technique

Ching-Chang Cho*, Ching-Huang Chiu, Kuo-Ching Chiu, Chong-You Lai

Department of Vehicle Engineering, National Formosa University, Taiwan

Abstract This study uses the heatline technique to estimate the natural convection heat transfer characteristics in an inclined wavy-wall cavity filled with Al_2O_3-water nanofluid. In this study cavity, it is assumed that the left and right walls have a wavy surface and are maintained at a high and low temperature, respectively. In addition, the upper and lower walls are both flat and insulated. The flow and temperature fields within the cavity are governed by the continuity equation, momentum equations, energy equation and Boussinesq approximation, and are solved numerically using the finite-volume method and SIMPLE algorithm. The results show that the inclination angle of the cavity has no significant effect on the heat function contours and Nusselt number for low Rayleigh numbers. However, given high Rayleigh numbers, the effect of inclination angle on heat function contours and Nusselt number is significant. In addition, the results also show that the Nusselt number increases as the Al_2O_3 nanoparticles is added to the working fluid.

Keywords Heatline, Nanofluid, Cavity, Wavy-wall, Natural convection

1. Introduction

Natural convection heat transfer in inclined cavities has many important applications in engineering systems, including solar energy collectors, double-glazed windows, car batteries, electronic cooling systems, crystal growth, and so on [1]. Thus, many researchers have investigated the flow field characteristics and heat transfer performance of natural convection in inclined cavities [2-4]. Overall, the results have shown that the flow conditions (e.g., Rayleigh number and Prandtl number) and geometry parameters (e.g., inclination angle and aspect ratio of cavity) have a significant effect on the flow characteristics and heat transfer behavior in the cavity. An optimal heat transfer performance occurs at a specific inclination angle of the cavity.

In many engineering applications, wavy geometry structures are often used to enhance the heat transfer performance within cavities, such as heat exchangers, solar collectors, cooling systems for microelectronic devices, underground cable systems, and so forth. Many studies have shown that the use of the wavy geometry structures can improve the heat transfer performance when wavy geometry parameters have appropriate values [5-7].

The heat transfer performance can also be improved by changing the thermophysical properties of the working fluid. Nanofluids, consisting of nanoparticles with high thermal conductivity (e.g., Al_2O_3 or Cu) suspended in a base fluid with low thermal conductivity (e.g., water or oil), provide an effective means of improving the thermophysical properties of the working fluid [8]. In recent years, many researchers have studied the problem of natural convection heat transfer in cavities filled with nanofluids [9-11]. Overall, the results have shown that the heat transfer performance increases with an increasing nanoparticle volume fraction. In addition, the type of nanoparticle added to the working fluid affects the heat transfer effect.

To show the path of heat transfer, a useful tool is the heatline visualization technique [12, 13]. Many researchers have used the technique to study the natural convection heat transfer characteristics in cavities [14-16]. These results have shown that the use of the heatline visualization technique can show and explain the heat transfer process in detail.

The present study investigates the natural convection heat transfer performance in an inclined wavy-wall cavity filled with Al_2O_3-water nanofluid using the heatline visualization technique. In modeling the cavity, the left and right walls are assumed to have a wavy surface and a high and low temperature, respectively, while the upper and lower walls are assumed to be flat and insulated. The flow behavior and heat transfer characteristics in the cavity are assumed to be governed by the continuity equation, momentum equations, energy equation and Boussinesq approximation. In performing the simulations, the governing equations are solved using the finite-volume method and the SIMPLE (semi-implicit method for pressure-linked equations) algorithm. The effects of the Rayleigh number, nanoparticle

* Corresponding author:
cccho@nfu.edu.tw (Ching-Chang Cho)
Published online at http://journal.sapub.org/jmea

volume fraction and cavity inclination angle on the heat function distribution and Nusselt number in the inclined wavy-wall cavity filled with Al_2O_3-water are examined.

2. Mathematical Formulation

2.1. Governing Equations

Figure 1 illustrates the studied cavity. As shown, the left and right walls have a wavy surface, while the top and bottom walls are flat. In addition, the width and height of this cavity are W_c and H_c, respectively. Furthermore, the cavity is inclined at an angle ϑ to the horizontal. The gravitational force (g) is assumed to act in the negative *y*-direction.

It is assumed that the used nanofluid is Newtonian and incompressible. The fluid flow in the cavity is assumed to be two-dimensional, laminar and steady state. In addition, the base fluid and nanoparticles are in thermal equilibrium and no relative motion occurs between them. Furthermore, the thermophysical properties of the nanofluid are all constant other than the density which varies in accordance with the Boussinesq approximation.

Let the following non-dimensional quantities be introduced:

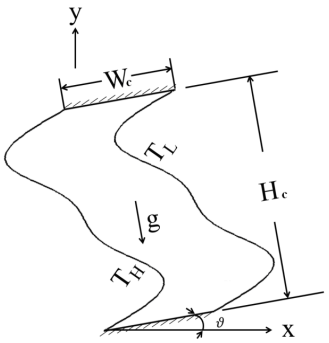

Figure 1. Schematic illustration of wavy wall cavity

$$\nabla^* = W_c\nabla,\ \vec{V}^* = \frac{\vec{V}}{\alpha_{bf}/W_c},$$
$$p^* = \frac{p-p_0}{\rho_{bf}\alpha_{bf}^2/W_c^2},\ \theta = \frac{T-T_L}{T_H-T_L} \quad (1)$$

where $\vec{V}$ is the velocity vector with components u and v in the *x*- and *y*-directions, respectively; α is the thermal diffusivity; p is the pressure; p_0 is the reference pressure; ρ is the density; θ is the dimensionless temperature; T is the temperature; T_H and T_L are the high temperature and low temperature, respectively; and the subscript bf indicates the base fluid (i.e., water). Under the conditions of ignoring thermal radiation and viscous dissipation effects, the governing equations described the flow and temperature fields have the following non-dimensionalized forms:

$$\nabla^* \cdot \vec{V}^* = 0, \quad (2)$$

$$(\vec{V}^* \cdot \nabla^*)\vec{V}^* = -\frac{\rho_{bf}}{\rho_{nf}}\nabla^* P^* + \frac{\nu_{nf}}{\nu_{bf}}\Pr\nabla^{*2}\vec{V}^* + Ra\cdot\Pr\cdot\frac{(1-\varphi)(\rho\beta)_{bf}+\varphi(\rho\beta)_p}{\rho_{nf}\beta_{bf}}\cdot\theta\cdot[Sin\vartheta\vec{i}+Cos\vartheta\vec{j}], \quad (3)$$

$$(\vec{V}^* \cdot \nabla^*\theta) = \frac{\alpha_{nf}}{\alpha_{bf}}\nabla^2\theta, \quad (4)$$

where the superscript * denotes a non-dimensional quantity; the subscripts nf and p denote the nanofluid and nanoparticles, respectively; $\nu(=\mu/\rho)$ is the kinematic viscosity; β is the thermal expansion coefficient; ϕ is the volume fraction of Al_2O_3 nanoparticles; $Ra(=\frac{g\beta_{bf}W_c^3(T_H-T_L)}{(\mu_{bf}/\rho_{bf})\alpha_{bf}})$ is the Rayleigh number; and $\Pr(=\frac{\mu_{bf}}{\alpha_{bf}\rho_{bf}})$ is the Prandtl number. In addition, the effective thermophysical properties of nanofluid presented in Eqs. (2)-(4) can be estimated as follows [17, 18]: density, $\rho_{nf} = (1-\phi)\rho_{bf} + \phi\rho_p$; viscosity, $\mu_{nf} = \frac{\mu_{bf}}{(1-\phi)^{2.5}}$; thermal diffusivity, $\alpha_{nf} = \frac{k_{nf}}{(\rho C_p)_{nf}}$; thermal conductivity, $\frac{k_{nf}}{k_{bf}} = \frac{(k_p+2k_{bf})-2\phi(k_{bf}-k_p)}{(k_p+2k_{bf})+\phi(k_{bf}-k_p)}$; and specific heat, $(\rho C_p)_{nf} = (1-\phi)(\rho C_p)_{bf} + \phi(\rho C_p)_p$. Furthermore, the Nusselt number (Nu) estimated the heat transfer performance can be defined in the non-dimensionalized form:

$$Nu = -\frac{k_{nf}}{k_{bf}}\left(\frac{\partial\theta}{\partial n^*}\right)_w. \quad (5)$$

Finally, the mean Nusselt number along the left wavy-wall surface can be obtained as:

$$Nu_m = \frac{1}{l_w^*}\int_0^{H_c^*} Nu\,dy, \quad (6)$$

where l_w^* is the non-dimensional length of the wavy-wall.

2.2. Boundary Conditions

As shown in Fig. 1, the left wall of the cavity is maintained at a constant high temperature, the right wall has a constant low temperature, and the top and bottom walls are both

insulated. A no-slip impermeable velocity boundary condition is assumed to apply at all of the wall surfaces. The dimensionless boundary conditions can be summarized as follows:

Left wall: $\vec{V}^* = 0,\ \theta = 1$

Right wall: $\vec{V}^* = 0,\ \theta = 0$

Top and bottom walls: $\vec{V}^* = 0,\ \partial\theta / \partial n^* = 0$

2.3. Heat Function

The energy equation in a two-dimensional, incompressible, and steady-state for nanofluid-filled cavity without heat generation can be written in the following non-dimensionalized form [12, 13]:

$$\frac{\partial J^*_{e,x}}{\partial x^*} + \frac{\partial J^*_{e,y}}{\partial y^*} = 0 \tag{7}$$

where $J^*_{e,x}[= \frac{(\rho C_p)_{nf}}{(\rho C_p)_{bf}} u^*\theta - \frac{k_{nf}}{k_{bf}} \frac{\partial\theta}{\partial x^*}]$ and $J^*_{e,y}[= \frac{(\rho C_p)_{nf}}{(\rho C_p)_{bf}} v^*\theta - \frac{k_{nf}}{k_{bf}} \frac{\partial\theta}{\partial y^*}]$ are the heat flux vector in x- and y- directions, respectively. Let the dimensionless heat function ($H^* = \frac{H}{k_{nf}\Delta T}$) be defined as follows:

$$\frac{\partial H^*}{\partial y^*} = J^*_{e,x} = \frac{(\rho C_p)_{nf}}{(\rho C_p)_{bf}} u^*\theta - \frac{k_{nf}}{k_{bf}} \frac{\partial\theta}{\partial x^*} \tag{8a}$$

$$-\frac{\partial H^*}{\partial x^*} = J^*_{e,y} = \frac{(\rho C_p)_{nf}}{(\rho C_p)_{bf}} v^*\theta - \frac{k_{nf}}{k_{bf}} \frac{\partial\theta}{\partial y^*} \tag{8b}$$

The heat function equation in the non-dimensionalized form can be obtained as:

$$\frac{\partial^2 H^*}{\partial x^{*2}} + \frac{\partial^2 H^*}{\partial y^{*2}} = \frac{(\rho C_p)_{nf}}{(\rho C_p)_{bf}} [\frac{\partial(u^*\theta)}{\partial y^*} - \frac{\partial(v^*\theta)}{\partial x^*}] \tag{9}$$

Note that the boundary conditions for the Eq. (9) can be obtained by integrating the Eq. (8).

2.4. Wavy-Wall Geometry and Numerical Solution Procedure

The non-dimensional profile of the wavy-wall was modeled as follows:

$$x^* = \alpha_w Sin(\pi y^*) + \frac{\alpha_w}{2.5} Sin(2\pi y^*), \tag{10}$$

where α_w is the wave amplitude.

The grid system of the wavy-wall cavity was generated by solving a set of Poisson equations [20]. A generalized coordinate transform technique was used to transform the governing equations from a Cartesian coordinate system to a generalized curvilinear coordinate system. The transformed governing equations have following generalized form [17-19]:

$$\begin{aligned} &\frac{\partial}{\partial\xi}(\rho_\varphi U f) + \frac{\partial}{\partial\eta}(\rho_\varphi V f) = \frac{\partial}{\partial\xi}[\frac{\Gamma_\varphi}{J}(\alpha_\varphi \frac{\partial f}{\partial\xi} - \beta_\varphi \frac{\partial f}{\partial\eta})] \\ &+ \frac{\partial}{\partial\eta}[\frac{\Gamma_\varphi}{J}(-\beta_\varphi \frac{\partial f}{\partial\xi} + \gamma_\varphi \frac{\partial f}{\partial\eta})] + JS_\varphi \end{aligned}, \tag{11}$$

where f is a generalized variable.

The finite-volume method [21] is used to discretize the governing equations and corresponding boundary conditions. The second-order upwind scheme is utilized to discretize the convection terms in the Eqs. (3) and (4). The SIMPLE algorithm [21] is used to couple the velocity-pressure fields. Finally, line-by-line TDMA (tri-diagonal matrix algorithm) iterative scheme is imposed to solve the discretized algebraic equations.

2.5. Grid-Independence Evaluation and Numerical Validation

The variations of the mean Nusselt number along the hot wavy-wall surface with the grid sizes of 51×101, 101×201, 101×401, and 201×801 are performed in the cavity with $\alpha_w = 0.5$, $\phi = 2\%$, $\vartheta = 0^\circ$ and $Ra = 10^6$. The obtained results have shown that a grid size of 101×401 has a grid-independent solution. The computational domain was thus meshed accordingly.

The present numerical results for the variation of the mean Nusselt number in an inclined square cavity with Pr = 100 have compared with those presented in [22]. Note that in the compared cavity, the top and bottom walls were maintained at low and high temperatures, respectively, while the left and right walls were assumed to be insulated. Table 1 presents the results. As shown, it is seen that the present results are consistent with those presented in [22].

Table 1. Comparison of present results for mean Nusselt number with published results

ϑ =	$Ra = 10^4$				$Ra = 10^5$			
	30°	45°	60°	90°	30°	45°	60°	90°
Present results	2.503	2.551	2.533	2.275	4.758	4.985	5.101	4.727
Khezzar *et al.* [22]	2.469	2.530	2.525	2.284	4.434	4.960	5.077	4.700

3. Results and Discussion

In the current study, the Al_2O_3-water nanofluid is used. The thermophysical properties of the Al_2O_3 nanoparticles are as follows [17-19]: $\rho = 3970 kg/m^3$, $k = 40 W/mK$, $C_p = 765 J/kgK$, and $\beta = 0.85\times10^{-5}/K$. The thermophysical properties of the water are as follows: $\rho = 997.1 kg/m^3$, $k = 0.613 W/mK$, $C_p = 4179 J/kgK$, and $\beta = 21\times10^{-5}/K$. In addition, the Prandtl number was set as $\Pr = 6.2$. The amplitude of the wavy surface is given $\alpha_w = 0.5$.

Figures 2 and 3 plot the heat function contours in the cavity given Rayleigh numbers of $Ra = 10^2$ and $Ra = 10^6$, respectively. Given a low Rayleigh number, since the flow velocity due to buoyancy force in the cavity is lower, the heat energy is transported slowly and more uniformly form the high temperature wall to low temperature wall for all considered nanoparticle volume fractions and inclination angles. As a result, a more uniform heat function contours without enclosed cell are presented in the cavity (see Fig. 2). Given a high Rayleigh number, since the flow velocity is high, the heat energy can be transported fast via the fluid flow for all considered nanoparticle volume fractions and inclination angles. Consequently, the heat function contours are more complex. It also shows that enclosed cells are presented in the cavity. This result indicates that the heat energy is rotated in the enclosed cells. Comparing the heat function contours between the two Rayleigh numbers, it is shown that higher values of heat function are presented in the case of the higher Rayleigh number. This result implies that the heat transfer is better in the case of the higher Rayleigh number. When the cavity is inclined, the direction of the gravitational force acting on the nanofluid changes, and prompts a corresponding change in the buoyancy effect. At low Rayleigh numbers, since the buoyancy effect is weak and the fluid flow is slow, there is no significant change in the heat function patterns. However, at high Rayleigh numbers, the buoyancy effect is strong and is thus susceptible to changes in the orientation of the cavity. Therefore, significant changes in the distribution of heat function contours occur as the inclination angle is varied.

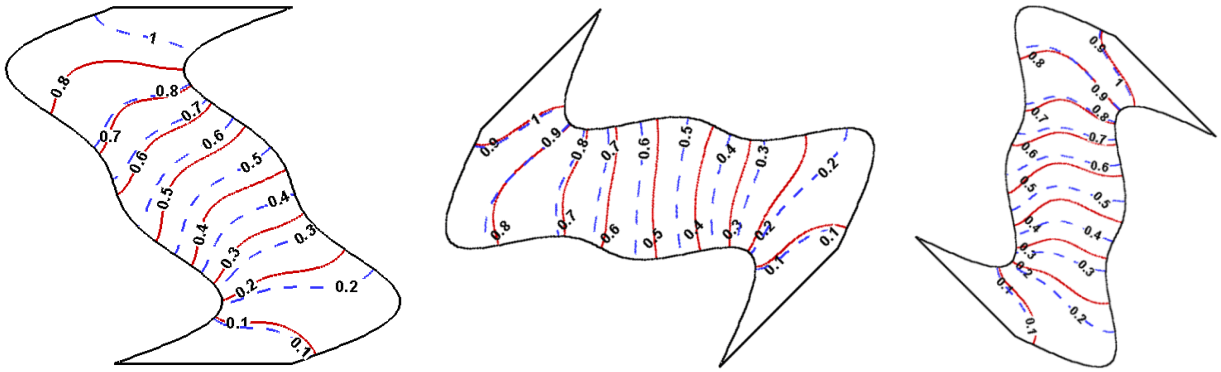

(a) (b) (c)

Figure 2. Distribution of heatlines in cavity given Rayleigh numbers of $Ra = 10^2$ and inclination angles of: (a) $\vartheta = 0^\circ$, (b) $\vartheta = 45^\circ$, and (c) $\vartheta = -45^\circ$. Note that solid line indicates $\phi = 0\%$, and dashed line indicates $\phi = 4\%$

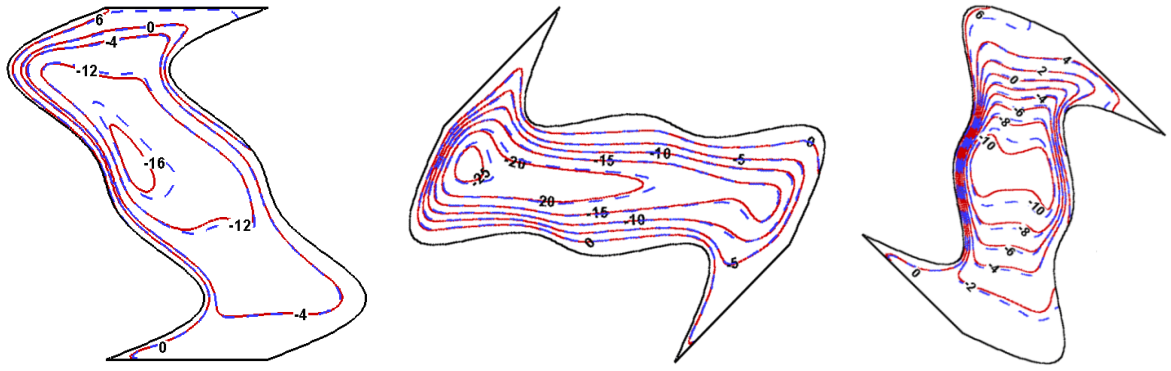

(a) (b) (c)

Figure 3. Distribution of heatlines in cavity given Rayleigh numbers of $Ra = 10^6$ and inclination angles of: (a) $\vartheta = 0^\circ$, (b) $\vartheta = 45^\circ$, and (c) $\vartheta = -45^\circ$. Note that solid line indicates $\phi = 0\%$, and dashed line indicates $\phi = 0\%$

Figure 4 shows the variation of the mean Nusselt number with the Rayleigh number as a function of the inclination angles. As discussed above, under low Rayleigh number conditions, the flow velocity and heat function have only slightly variation for all inclination angles. Consequently, an approximately constant mean Nusselt number is obtained for all inclination angles. However, as the Rayleigh number increases, the strength of the heat function is increased and enclosed cells are presented in the cavity. The results indicate that a stronger heat energy transport occurs. Therefore, the mean Nusselt number increases as the Rayleigh number increased. In addition, for high Rayleigh numbers, a significant change in the distribution of the heat function occurs when the cavity is inclined. Consequently, the mean Nusselt number have also significant variation as the cavity is inclined.

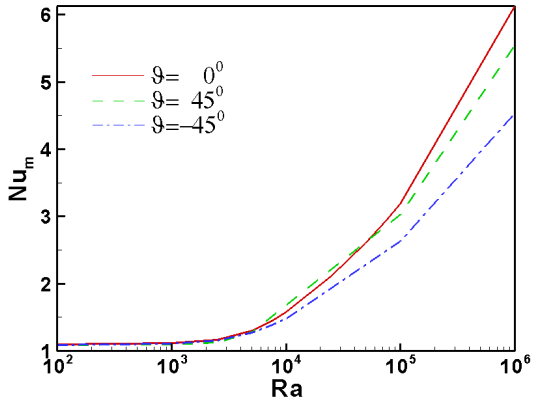

Figure 4. Variation of mean Nusselt number with Rayleigh number as function of inclination angle. Note that $\varphi = 4\%$

Figure 5 shows the variation of the mean Nusselt number with the Rayleigh number as a function of nanoparticle volume fractions. Since the Al_2O_3 nanoparticles add to the water, the thermal conductivity of working fluid is added. As a result, the heat energy can be transported fast. Consequently, it is shown that the mean Nusselt number increases as the volume fraction of Al_2O_3 nanoparticle for all considered Rayleigh number.

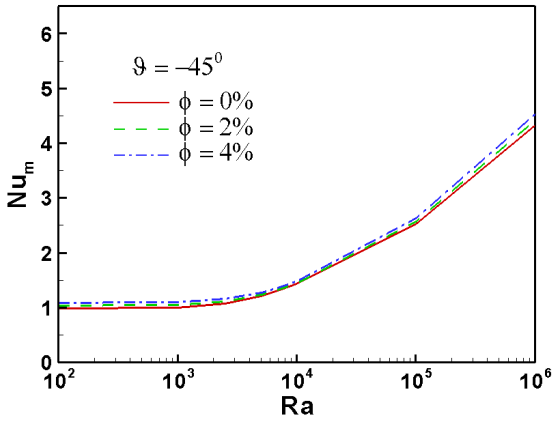

Figure 5. Variation of mean Nusselt number with Rayleigh number as function of nanoparticle volume fraction. Note that $\vartheta = -45^{\circ}$

4. Conclusions

This study has used the heatline technique to estimate the natural convection heat transfer performance of Al_2O_3-water nanofluid in a cavity bounded by vertical isothermal walls with a wavy surface and straight upper and lower walls with adiabatic conditions. In performing the simulations, the governing equations have been modeled using the continuity equation, momentum equations, energy equation and Boussinesq approximation, and then solved numerically using the finite volume method and SIMPLE algorithm. The results have shown that the distribution of heat function in the cavity is strongly dependent on the inclination angle of the cavity for higher Rayleigh numbers. However, given low Rayleigh numbers, the inclination angle has no significant effect on heat function contours and Nusselt number. In addition, the results have also shown that the use of nanofluid can increase the Nusselt number.

ACKNOWLEDGEMENTS

The authors would like to thank the Ministry of Science and Technology, Taiwan, R.O.C. for the financial support of this study under Contract No. MOST 104-2221-E-150-045.

REFERENCES

[1] Singh, A.K., Roy, & S., Basak, T. (2012). Analysis of Bejan's heatlines on visualization of heat flow and thermal mixing in titled square cavity. *International Journal of Heat and Mass Transfer*, 55, 2965-2983.

[2] Rahman, M., & Sharif, M.A.R. (2003). Numerical study of laminar natural convection in inclined rectangular enclosures of various aspect ratios. *Numerical Heat Transfer, Part A: Applications*, 44, 355-373.

[3] Huelsz, G., & Rechtman, R. (2013). Heat transfer due to natural convection in an inclined square cavity using the lattice Boltzmann equation method. *International Journal of Thermal Sciences*, 65, 111-119.

[4] Omranian, A., Craft, T.J., & Iacovides, H. (2014). The computation of buoyant flows in differentially heated inclined cavities. *International Journal of Heat and Mass Transfer*, 77, 1-16.

[5] Dalal, A., & Das, M.K. (2006). Natural convection in a cavity with a wavy wall heated from below and uniformly cooled from the top and both sides. *ASME Journal of Heat Transfer*, 128, 717-725.

[6] Oztop, H.F., Abu-Nada, E., Varol, Y., & Chamkha, A. (2011). Natural convection in wavy enclosures with volumetric heat sources. *International Journal of Thermal Sciences*, 50, 502-514.

[7] Hasan, M.N., Saha, S., & Saha, S.C. (2012). Effects of corrugation frequency and aspect ratio on natural convection within an enclosure having sinusoidal corrugation over a heated top surface. *International Communications in Heat*

and Mass Transfer, 39, 368-377.

[8] Yu, W., France, D.M., Routbirt, J.L., & Choi, S.U.S. (2008). Review and comparison of nanofluid thermal conductivity and heat transfer enhancements. *Heat Transfer Engineering*, 29, 432-460.

[9] Oztop, H.F., & Abu-Nada, E. (2008). Numerical study of natural convection in partially heated rectangular enclosures filled with nanofluids. *International Journal of Heat and Fluid Flow*, 29, 1326-1336.

[10] Abouali, O. & Ahmadi, G. (2012). Computer simulations of natural convection of single phase nanofluids in simple enclosures: A critical review. *Applied Thermal Engineering*, 36, 1-13.

[11] Sidik, N.A.C., & Razali, S.A. (2014). Lattice Boltzmann method for convective heat transfer of nanofluids - A review. *Renewable and Sustainable Energy Reviews*, 38, 864-875.

[12] Kimura, S., & Bejan, A. (1983). The "Heatline" visualization of convective heat transfer. *ASME Journal of Heat Transfer*, 105, 916-919.

[13] Casta, V.A.F. (2006). Bejan's heatlines and masslines for convection visualization and analysis. *ASME Applied Mechanics Reviews*, 59, 126-145.

[14] Oztop, H.F., Mobedi, M., Abu-Nada, E., & Pop, I. (2012). A heatline analysis of natural convection in a square inclined enclosure filled with a CuO nanofluid under non-uniform wall heating condition. *International Journal of Heat and Mass Transfer*, 55, 5076-5086.

[15] Basak, T., & Chamkha, A.J. (2012). Heatline analysis on natural convection for nanofluids confined within square cavities with various thermal boundary conditions. *International Journal of Heat and Mass Transfer*, 55, 5526-5543.

[16] Sheikholeslami, M., Gorji-Bandpy, M., & Soleimani, S. (2013). Two phase simulation of nanofluid flow and *heat transfer using heatline analysis.* International Communications in Heat and Mass Transfer, 47, 73-81.

[17] Cho, C.C., Chen, C.L., & Chen, C.K. (2013). Mixed convection heat transfer performance of water-based nanofluid in lid-driven cavity with wavy surfaces. *International Journal of Thermal Sciences*, 68, 181-190.

[18] Cho, C.C., Chen, C.L., & Chen, C.K. (2013). Natural convection heat transfer and entropy generation in wavy-wall enclosure containing water-based nanofluid. *International Journal of Heat and Mass Transfer*, 61, 749-758.

[19] Cho, C.C. (2014). Heat transfer and entropy generation of natural convection in nanofluid-filled square cavity with partially-heated wavy surface. *International Journal of Heat and Mass Transfer*, 77, 818-827.

[20] Thomas, P.D., & Middlecoff, J.F. (1980). Direct control of the grid point distribution in meshes generated by elliptic equations. *AIAA Journal*, 18, 652-656.

[21] Patankar, S.V. (1980) *Numerical Heat Transfer and Fluid Flow*, New York, McGraw-Hill.

[22] Khezzar, L., Siginer, D., & Vinogradov, I. (2012). Natural convection of power law fluids in inclined cavities. *International Journal of Thermal Sciences*, 53, 8-17.